engineering proceedings

MDPI

Proceeding Paper

Nondestructive Quality Evaluation of Nakhon Phanom Lychee (NP.1) Using Parallel Coupled Line Microstrip via Isolation Loss Parameter Analysis †

Decha Wongpatsa [1], Kritphon Phanrattanachai [2], Siriwat Ninlawat [3], Phatcharanat Saeng-On [4], Niwat Angkawisittpan [5], Somchat Sonasang [6,*] and Ravee Phomloungsri [7]

[1] Interdisciplinary Studies Program, Faculty of Agriculture and Technology, Nakhon Phanom University, Nakhon Phanom 48000, Thailand; decha@npu.ac.th
[2] Department of Electronics and Automation Systems Engineering, Faculty of Agricultural and Industrial Technology, Phetchabun Rajabhat University, Phetchabun 67000, Thailand; kritphon.ai@pcru.ac.th
[3] Department of Electrical Technology, Faculty of Industrial Technology, Nakhon Phanom University, Nakhon Phanom 48000, Thailand; siriwut.n@npu.ac.th
[4] Department of Electronics and Intelligent Robotics Engineering, Faculty of Industrial Technology, Nakhon Phanom University, Nakhon Phanom 48000, Thailand; s.phatcharanat@npu.ac.th
[5] Research Unit for Electrical and Computer Engineering, Faculty of Engineering, Mahasarakham University, Maha Sarakham 44150, Thailand; niwat.a@msu.ac.th
[6] Electrical Elements and Wireless Devices Unit (EEWDU), Faculty of Industrial Technology, Nakhon Phanom University, Nakhon Phanom 48000, Thailand
[7] Department of Computer and Communication Engineering, Faculty of Technology and Engineering, Udon Thani Rajabhat University, Udon Thani 41000, Thailand; ravee.ph@udru.ac.th
* Correspondence: somchat.s@npu.ac.th
† Presented at the 13th International Electronic Conference on Sensors and Applications, 18–20 November 2026; Available online: https://sciforum.net/event/ECSA-13.

Abstract

This study investigates the isolated-port response of a four-port parallel coupled-line microstrip structure as a nondestructive microwave indicator for storage-related changes in Nakhon Phanom Lychee (NP.1). Unlike conventional one-port or two-port microwave sensors that mainly rely on reflection, forward transmission, resonant-frequency shift, or quality factor, the present approach monitors the nominally isolated port, where the measured signal is affected by perturbation of the coupled-line field balance. Ten fruits were stored under refrigerated conditions and evaluated at 7-day intervals over three storage periods. Each fruit was measured ten times during each period at room temperature using a two-port vector network analyzer over 0.3–0.8 GHz. In the adopted connection, the measured VNA S_{21} corresponded to the sensor isolated-port parameter S_{31}. The mean resonant frequency decreased from 487 MHz in Week 1 to 478 MHz in Weeks 2 and 3. The S_{31} magnitude at the resonant dip became progressively less negative, changing from −59.59 dB to −53.95 dB and −48.27 dB, corresponding to a total change of 11.32 dB. Although the resonant frequency did not distinguish Weeks 2 and 3, the isolation magnitude remained different between these periods. The measured response is consistent with storage-related changes in the effective electromagnetic properties of the fruit. These preliminary results support the feasibility of using isolated-port magnitude as an additional microwave feature for nondestructive lychee monitoring. Further validation using direct physicochemical, dielectric, and metrological measurements is required before quantitative quality assessment can be established.

Check for updates

Academic Editor: Jean-Marc Laheurte

Published: 30 October 2026

Copyright: © 2026 by the authors. Licensee MDPI, Basel, Switzerland. This article is an open access article distributed under the terms and conditions of the Creative Commons Attribution (CC BY) license.

 https://doi.org/10.3390/engproc2026163049

Keywords: nondestructive evaluation; Nakhon Phanom Lychee; parallel coupled-line microstrip; S31 parameter; isolated-port response; dielectric sensing; post-harvest monitoring; microwave sensor

1. Introduction

Post-harvest quality changes affect the appearance, storage life, and market value of fresh fruit. Conventional assessment commonly relies on visual inspection, firmness testing, weight-loss measurement, soluble-solids analysis, or chemical testing. Although these methods provide useful information, several require sample preparation or destruction and are unsuitable for repeated measurements of the same fruit. Nondestructive techniques based on optical, acoustic, electromagnetic, dielectric, and gas-sensing principles have therefore been investigated for fruit-quality assessment [1].

Lychee is highly susceptible to post-harvest deterioration. Xiong et al. used hyperspectral imaging to detect small surface damage and classify the condition of lychee fruit [2]. Yang et al. subsequently applied hyperspectral imaging to evaluate pericarp browning associated with moisture content [3] and to estimate anthocyanin content during storage [4]. More recently, Kanwal et al. showed that spectral information obtained from intact lychee surfaces could be related to quality parameters such as soluble solids, acidity, and mineral content [5]. Zhao et al. also combined hyperspectral, X-ray, and visible/near-infrared data for nondestructive detection of litchi stem borers [6]. These studies demonstrate the usefulness of nondestructive sensing for lychee. However, optical and multisensor systems generally require controlled illumination, calibration, image processing, and multivariate analysis.

Dielectric sensing provides another approach because the interaction between electromagnetic fields and fruit depends on complex permittivity. For fruits and vegetables, dielectric properties are affected by water content, soluble solids, tissue structure, and other physicochemical characteristics [7]. Lin et al. used dielectric characteristics to estimate quality parameters of golden passion fruit [8]. Bing et al. developed a flexible microwave resonator for nondestructive water-content sensing in fruits through changes in resonant response [9]. In another food application, Khoshchehre et al. used a microstrip sensor and the measured transmission response to detect milk spoilage [10]. These studies indicate that microwave structures can detect changes in high-moisture biological materials without cutting or chemically treating the sample.

Planar microstrip sensors are attractive because they are compact, inexpensive, and readily connected to a vector network analyzer. Most reported microwave sensors for food and agricultural applications use one-port or two-port configurations. In these configurations, S_{11} is commonly interpreted through impedance mismatch, resonant-frequency shift, or return-loss variation, while S_{21} is usually interpreted through forward transmission, insertion loss, or attenuation through the sensing region. These parameters are useful, but they do not directly exploit the isolated-port behavior that is available in a four-port coupled-line network.

A four-port parallel coupled-line architecture was selected in this study because it provides through, coupled, and isolated responses from the same sensing region. In an ideal directional coupled-line network, the isolated port receives only a very small signal because of modal balance between the even- and odd-mode fields. When a dielectric object is placed near the coupled section, the fringing fields are perturbed and the effective modal propagation constants and losses are altered. This perturbation can disturb the cancellation condition at the isolated port and produce a measurable change in the isolation magnitude. Thus, the four-port structure is more complex than a one-port or two-port resonator, but it

offers an additional sensing feature that is not available when only reflection or forward transmission is measured.

Morales-Lovera et al. used coupled microstrip resonators to determine complex anisotropic permittivity from changes in resonant frequency and quality factor [11]. Rahimian Omam et al. showed that the coupled-port and isolated-port responses of a high-directivity coupled-line structure varied with the dielectric constant of the material under test [12]. Parallel coupled-line structures have also been applied to agricultural and food materials. Karasaeng et al. related the transmission response of a parallel-coupled-line band-stop structure to fermented fish samples [13], while Phanomupatum et al. used coupled microstrip lines for non-invasive rice-moisture measurement [14]. These studies support the use of microstrip and coupled-line perturbation for dielectric sensing, but the use of the isolated-port response as the primary feature for monitoring lychee storage remains limited.

Despite these developments, nondestructive studies of lychee have mainly relied on optical imaging and multi-sensor systems. Microwave coupled-line sensors have been applied mostly to other fruits, grains, foods, and reference dielectric materials. Moreover, most microwave sensing studies focus on reflection, forward transmission, resonant-frequency shift, or quality factor. It remains unclear whether the isolated-port magnitude of a four-port parallel coupled-line microstrip structure can distinguish successive storage periods when the resonant frequency remains unchanged.

This study investigates a four-port parallel coupled-line microstrip structure for nondestructive monitoring of Nakhon Phanom Lychee (NP.1) during refrigerated storage. The isolation response, represented by S_{31}, was measured over 0.3–0.8 GHz for ten fruits during three storage periods. Each fruit was measured ten times in each period. The analysis considered both resonant-frequency shift and isolation magnitude. The main contribution is the evaluation of the isolated-port magnitude as an additional microwave indicator when resonant-frequency shift alone cannot separate successive storage conditions. Since moisture content, firmness, soluble solids, and dielectric properties were not measured independently, the present work is treated as an initial feasibility study of storage-related electromagnetic changes in lychee.

2. Materials and Methods

2.1. Four-Port Parallel Coupled-Line Microstrip Structure

For a four-port network, the relationship between the incident and reflected waves is expressed as

$$\begin{bmatrix} b_1 \\ b_2 \\ b_3 \\ b_4 \end{bmatrix} = \begin{bmatrix} S_{11} & S_{12} & S_{13} & S_{14} \\ S_{21} & S_{22} & S_{23} & S_{24} \\ S_{31} & S_{32} & S_{33} & S_{34} \\ S_{41} & S_{42} & S_{43} & S_{44} \end{bmatrix} \begin{bmatrix} a_1 \\ a_2 \\ a_3 \\ a_4 \end{bmatrix}, \tag{1}$$

where a_n and b_n denote the incident and reflected waves at Port n, respectively. When Port 1 is excited and the remaining ports are terminated with matched 50-Ω loads, the isolated-port response is defined as

$$S_{31} = \left. \frac{b_3}{a_1} \right|_{a_2=a_3=a_4=0}. \tag{2}$$

The magnitude of the isolation response in decibels is given by

$$S_{31,\mathrm{dB}}(f) = 20 \log_{10} |S_{31}(f)|. \tag{3}$$

https://doi.org/10.3390/engproc2026163049

The sensing structure consisted of two parallel microstrip transmission lines fabricated on an FR-4 substrate, as shown in Figure 1. The prototype geometry was adopted from a previous coupled-line microwave sensor study [14]; however, the present work uses the structure for a different sensing purpose. The structure was selected because its four-port configuration permits the isolated-port response to be observed while the remaining ports are terminated. This enables the fruit-induced perturbation of the coupled-line field balance to be examined through S_{31} rather than relying only on conventional S_{11} or S_{21} responses.

The central parallel-line section formed the sensing region. Port 1 was assigned as the input port, Port 2 as the coupled port, Port 3 as the isolated port, and Port 4 as the through port. With Port 1 used as the excitation port, the isolated-port response of the sensor was represented by S_{31}.

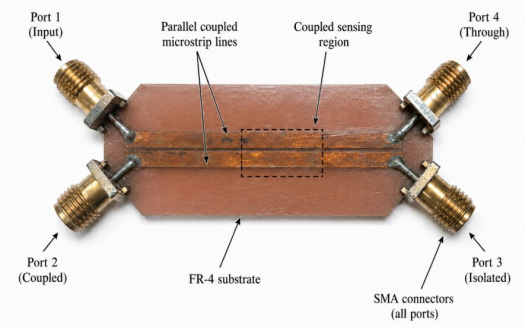


Figure 1. Fabricated four-port parallel coupled-line microstrip structure and port configuration: Port 1, input port; Port 2, coupled port; Port 3, isolated port; and Port 4, through port.

The sensing mechanism is based on perturbation of the coupled-line fringing fields by the lychee sample. In a coupled-line network, the isolation response depends on the balance between even- and odd-mode propagation. The effective permittivity and dielectric loss of a nearby fruit can alter the modal phase velocities and attenuation constants, thereby changing the cancellation condition at the isolated port. A change in S_{31} therefore indicates a change in the electromagnetic interaction between the fruit and the coupled sensing region.

Although the sensing structure was a four-port network, the measurements were performed using a two-port vector network analyzer. VNA Port 1 was connected to Sensor Port 1, whereas VNA Port 2 was connected to Sensor Port 3. Sensor Ports 2 and 4 were terminated with matched 50-Ω loads. Under this connection, the forward transmission parameter recorded by the VNA corresponds to the isolated-port response of the sensor:

$$S_{21}^{\mathrm{VNA}} = S_{31}^{\mathrm{sensor}}. \tag{4}$$

For consistency, all measured responses are reported as S_{31} throughout this paper.

2.2. Lychee Samples and Storage Procedure

Nakhon Phanom Lychee cultivar NP.1 was obtained from local growers in Nakhon Phanom Province, Thailand. Ten fruits with comparable size, maturity, and external appearance were selected for the experiment. Fruits with visible cracks, bruises, fungal growth, or other surface defects were excluded.

Before microwave measurement, the diameter of each fruit was measured using a digital vernier caliper. Figure 2 shows a representative fruit with a measured diameter of 24.92 mm.

The same ten fruits were used throughout the three-week experiment. Between measurement sessions, the samples were stored in a refrigerator at approximately 5 °C. Measure-

ments were performed at 7-day intervals. Week 1 represented the initial reference condition, followed by Weeks 2 and 3.

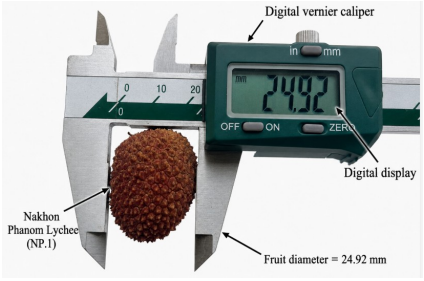


Figure 2. Nakhon Phanom Lychee (NP.1) sample and diameter measurement using a digital vernier caliper.

For each measurement session, the fruits were removed from refrigerated storage and measured under laboratory room-temperature conditions. The samples remained outside the refrigerator only during the measurement period and were returned immediately to refrigerated storage after all measurements had been completed. No cutting, peeling, puncturing, or chemical treatment was applied to the fruits. Before each measurement session, the fruit surfaces were inspected and gently cleaned to remove dust or foreign material.

2.3. Measurement Configuration and Metrological Control

The experimental setup is shown in Figure 3. A Keysight E5062A (Keysight Technologies, Santa Rosa, CA, USA) vector network analyzer was used to measure the scattering response over the frequency range from 0.3 to 0.8 GHz.

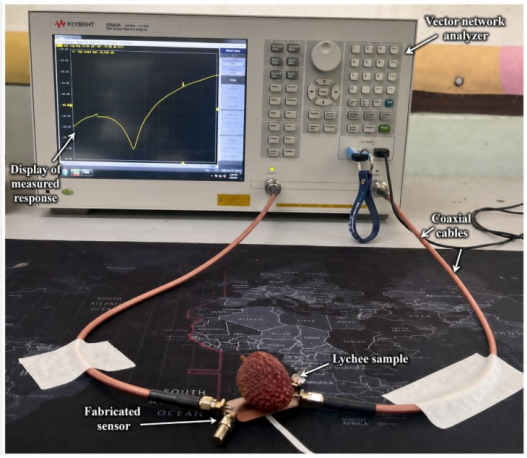


Figure 3. Experimental setup for measuring the isolated-port response of the parallel coupled-line microstrip structure using a Keysight E5062A vector network analyzer.

Before measurement, the vector network analyzer was calibrated at the ends of the coaxial cables using a short-open-load-through calibration procedure. Port 1 of the sensor was connected to the source port of the vector network analyzer, while Port 3 was connected to the receiving port. Ports 2 and 4 were terminated with matched 50-Ω loads.

Each fruit was placed at the center of the coupled sensing region using the same positioning procedure. Each of the ten fruits was measured ten times during each storage period. The fruit was removed and repositioned before each repeated measurement, and a 2-min interval was maintained between successive measurements. This repeated removal and repositioning was included to check the influence of positioning uncertainty on the measured response.

The ten responses obtained from each fruit were averaged to represent its response during that storage period. Thus, 100 measurements were obtained during each period and 300 measurements were obtained over the three storage periods. The mean response of the kth fruit during storage period i was calculated as

$$\overline{S}_{31,k,i}(f) = \frac{1}{N}\sum_{n=1}^{N} S_{31,k,i,n}(f), \qquad N = 10, \tag{5}$$

where $S_{31,k,i,n}(f)$ is the nth repeated response. When raw repeated-measurement data are available, the corresponding standard deviation can be calculated as

$$s_{31,k,i}(f) = \sqrt{\frac{1}{N-1}\sum_{n=1}^{N}\left[S_{31,k,i,n}(f) - \overline{S}_{31,k,i}(f)\right]^2}. \tag{6}$$

The present proceeding reports averaged S_{31} responses and discusses repeatability, sample repositioning, and temperature as metrological considerations. These aspects of the measurement protocol are summarized in Table 1. A more complete future study should report the standard deviation of both resonant frequency and resonant-dip magnitude, as well as controlled tests on sample position and temperature variation.

Table 1. Metrological considerations included in the experimental workflow.

Factor	Implementation in This Study	Purpose
Repeatability	Ten repeated measurements per fruit per period	Reduces random measurement variation
Sample repositioning	Fruit removed and repositioned before each repeat	Checks sensitivity to placement uncertainty
Sample variability	Ten fruits measured during each period	Includes biological variation among fruits
Temperature condition	Refrigerated storage and room-temperature measurement	Maintains a consistent measurement protocol
Port termination	Unused sensor ports terminated with 50-Ω loads	Reduces unwanted reflections and coupling error

3. Results

Figure 4 presents the measured S_{31} responses of the ten Nakhon Phanom Lychee (NP.1) fruits during Weeks 1, 2, and 3. Each curve represents one fruit and was obtained by averaging ten repeated measurements. The responses exhibited a similar overall pattern over the frequency range from 0.3 to 0.8 GHz, with the main difference appearing near the resonant dip around 0.47–0.50 GHz.

The Week 1 responses showed the deepest resonant dip. In Week 2, the dip shifted toward a lower frequency and became less negative. In Week 3, the resonant frequency remained close to that of Week 2, while the isolation magnitude continued to increase in the isolated-port response. These results indicate that the resonant region is the most responsive part of the measured response for distinguishing storage conditions.

Figure 5 compares the mean S_{31} responses of the three storage periods. The mean resonant frequency decreased from 0.487 GHz in Week 1 to 0.478 GHz in Week 2 and remained at approximately 0.478 GHz in Week 3. The corresponding S_{31} magnitude at the resonant dip changed from −59.59 dB in Week 1 to −53.95 dB in Week 2 and −48.27 dB in Week 3.

The extracted resonant frequency and isolated-port magnitude are summarized in Table 2. The resonant-frequency shift was effective for distinguishing Week 1 from the later storage periods. However, it could not separate Weeks 2 and 3 because both periods exhibited nearly the same resonant frequency. In contrast, the S_{31} magnitude remained different for all three periods. The magnitude change relative to Week 1 was 5.64 dB in Week 2 and 11.32 dB in Week 3. The additional difference between Weeks 2 and 3 was 5.68 dB.

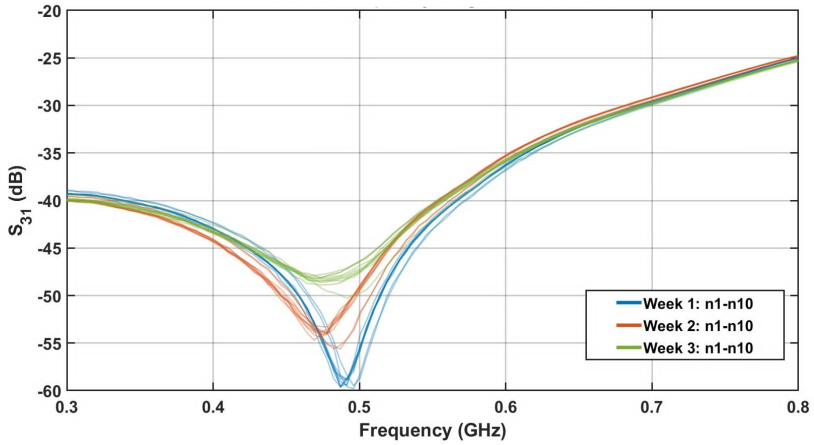


Figure 4. Measured S_{31} responses of ten Nakhon Phanom Lychee (NP.1) fruits during Weeks 1, 2, and 3. Each curve represents the mean of ten repeated measurements obtained from one fruit.

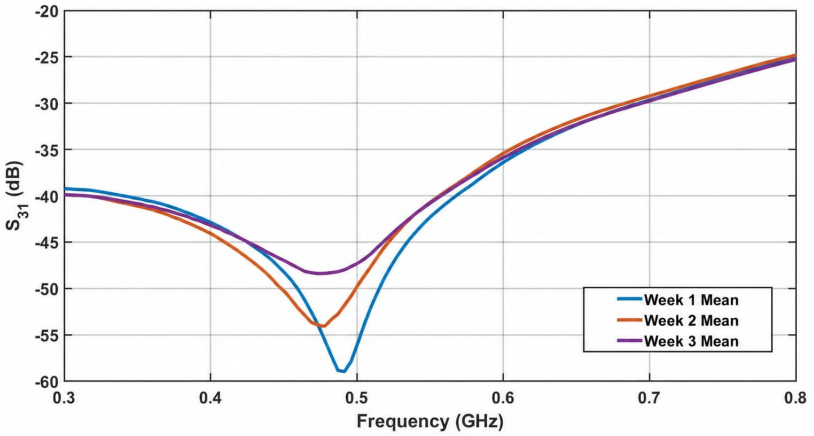


Figure 5. Comparison of the mean S_{31} responses obtained during Weeks 1, 2, and 3.

Table 2. Extracted resonant frequency and isolated-port magnitude during three storage periods.

Storage Period	Resonant Frequency (MHz)	Frequency Shift (MHz)	S_{31} at Resonant Dip (dB)	Magnitude Change (dB)
Week 1	487	0	−59.59	0
Week 2	478	−9	−53.95	5.64
Week 3	478	−9	−48.27	11.32

These results indicate that the isolated-port magnitude provides additional sensing information and can complement frequency-based analysis in monitoring storage-related changes in lychee. In particular, S_{31} magnitude distinguished Weeks 2 and 3 even though the resonant frequency remained unchanged.

4. Discussion

The results show that the four-port coupled-line response provides two related but different indicators: resonant-frequency shift and isolated-port magnitude. The frequency shift from 487 to 478 MHz indicates that the electromagnetic loading of the sensing region changed between Weeks 1 and 2. However, the absence of an additional frequency shift between Weeks 2 and 3 suggests that frequency tracking alone was not sufficient to separate the later storage periods under the present experimental conditions.

The isolated-port magnitude provided a clearer temporal distinction in this dataset. The measured S_{31} value became progressively less negative from Week 1 to Week 3, indicating that a stronger signal appeared at the nominally isolated port. From the viewpoint of a coupled-line network, this represents a reduction in isolation. From the viewpoint of sensing, however, the change is useful because it reflects a perturbation of the modal balance in the coupled region.

This behavior is consistent with the expected operation of a coupled-line sensor. The presence of the fruit near the coupled section changes the local effective permittivity and dielectric loss experienced by the fringing fields. During refrigerated storage, lychee fruit may undergo moisture redistribution, mass loss, respiration-related changes, tissue softening, and changes in soluble constituents. These processes can alter the effective dielectric behavior of the fruit and therefore the interaction between the sample and the sensor. Because no independent measurements of moisture content, firmness, soluble solids, or complex permittivity were included in this preliminary experiment, the observed S_{31} variation should be interpreted as an indicator of combined storage-related electromagnetic change rather than a direct measurement of a single quality parameter.

The main advantage of the four-port structure is that it offers an additional response channel compared with conventional one-port or two-port resonators. A one-port resonator mainly provides reflection and impedance information, whereas a two-port resonator mainly provides forward transmission and attenuation information. In contrast, a four-port coupled-line structure can use the isolated-port signal, which is sensitive to small disturbances of coupling balance. This provides a technical justification for using the more complex four-port architecture in applications where the resonant-frequency shift alone may become unchanged.

The present study also has metrological limitations. Although repeated measurements and sample repositioning were included in the workflow, numerical standard deviations, controlled positional offsets, and controlled temperature-dependence tests were not yet fully reported. Future work should therefore quantify the repeatability of resonant frequency and S_{31} magnitude, evaluate the effect of fruit position and orientation, and investigate the influence of measurement temperature. Direct comparison with S_{11} and conventional S_{21} features under the same experimental conditions would also be required to determine whether the isolated-port response provides superior sensitivity, robustness, or accuracy.

For practical lychee quality monitoring, the proposed method could be used as a rapid nondestructive screening tool during refrigerated storage. The isolated-port magnitude may serve as one feature in a multi-parameter microwave assessment system, together with resonant frequency, reflection, transmission, and possibly phase information. With further calibration against physicochemical quality indicators, the method could support storage monitoring, batch screening, and smart post-harvest management of lychee and other high-moisture fruits.

5. Conclusions

The isolated-port response of the parallel coupled-line microstrip structure provided a practical means of distinguishing storage-related changes in Nakhon Phanom Lychee

(NP.1). The main finding was that the S_{31} magnitude continued to change even when the resonant frequency no longer shifted. Therefore, isolated-port magnitude can complement frequency-based analysis and may provide an additional sensing feature for four-port microwave structures.

The contribution of this work is not the general use of microwave propagation for moisture-sensitive materials, but the evaluation of the nominally isolated port of a coupled-line structure as a post-harvest monitoring parameter. The proposed method is suitable as an initial nondestructive screening approach. However, further validation against measured physicochemical quality parameters, dielectric properties, repeatability statistics, positional sensitivity, and temperature effects is required before it can be applied to quantitative fruit-quality assessment.

Author Contributions: Conceptualization, D.W., P.S.-O. and S.S.; methodology, D.W., S.N., P.S.-O., N.A. and S.S.; software, K.P. and R.P.; validation, D.W., S.N. and P.S.-O.; formal analysis, K.P., N.A., S.S. and R.P.; investigation, D.W., S.N. and P.S.-O.; resources, D.W., P.S.-O. and S.S.; data curation, D.W., K.P. and R.P.; writing—original draft preparation, D.W., K.P. and P.S.-O.; writing—review and editing, N.A., S.S. and R.P.; supervision, N.A. and S.S. All authors have read and agreed to the published version of the manuscript.

Funding: This research received no external funding. The APC was funded by Decha Wongpatsa.

Institutional Review Board Statement: Not applicable.

Informed Consent Statement: Not applicable.

Data Availability Statement: The data presented in this study are available from the corresponding author upon reasonable request.

Acknowledgments: The authors would like to thank the Faculty of Industrial Technology, Nakhon Phanom University, for providing laboratory facilities and technical support for the microwave measurements. The authors also acknowledge the local lychee growers in Nakhon Phanom Province for supporting the collection of Nakhon Phanom Lychee (NP.1) samples used in this study.

Conflicts of Interest: The authors declare no conflicts of interest.

References

1. Liu, J.; Sun, J.; Wang, Y.; Liu, X.; Zhang, Y.; Fu, H. Non-Destructive Detection of Fruit Quality: Technologies, Applications and Prospects. *Foods* **2025**, *14*, 2137. [CrossRef]
2. Xiong, J.; Lin, R.; Bu, R.; Liu, Z.; Yang, Z.; Yu, L. A Micro-Damage Detection Method of Litchi Fruit Using Hyperspectral Imaging Technology. *Sensors* **2018**, *18*, 700. [CrossRef]
3. Yang, Y.-C.; Sun, D.-W.; Wang, N.-N. Rapid Detection of Browning Levels of Lychee Pericarp as Affected by Moisture Contents Using Hyperspectral Imaging. *Comput. Electron. Agric.* **2015**, *113*, 203–212. [CrossRef]
4. Yang, Y.-C.; Sun, D.-W.; Pu, H.; Wang, N.-N.; Zhu, Z. Rapid Detection of Anthocyanin Content in Lychee Pericarp during Storage Using Hyperspectral Imaging Coupled with Model Fusion. *Postharvest Biol. Technol.* **2015**, *103*, 55–65. [CrossRef]
5. Kanwal, N.; Kämper, W.; Farrar, M.B.; Tootoonchy, M.; Lynch, C.; Nichols, J.; Wallace, H.M.; Trueman, S.J.; Hosseini Bai, S. Rapid Assessment of Lychee and Mango Fruit Quality Using Hyperspectral Imaging. *LWT* **2025**, *224*, 117833. [CrossRef]
6. Zhao, Z.; Xu, S.; Lu, H.; Liang, X.; Feng, H.; Li, W. Nondestructive Detection of Litchi Stem Borers Using Multi-Sensor Data Fusion. *Agronomy* **2024**, *14*, 2691. [CrossRef]
7. El Khaled, D.; Novas, N.; Gazquez, J.A.; Garcia, R.M.; Manzano-Agugliaro, F. Fruit and Vegetable Quality Assessment via Dielectric Sensing. *Sensors* **2015**, *15*, 15363–15397. [CrossRef]
8. Lin, F.; Chen, D.; Liu, C.; He, J. Non-Destructive Detection of Golden Passion Fruit Quality Based on Dielectric Characteristics. *Appl. Sci.* **2024**, *14*, 2200. [CrossRef]
9. Bing, S.; Chawang, K.; Chiao, J.-C. A Tuned Microwave Resonator on Flexible Substrate for Nondestructive Water Content Sensing in Fruits. *IEEE J. Sel. Areas Sens.* **2024**, *1*, 93–104. [CrossRef]
10. Khoshchehre, A.; Sattari, M.A.; Shah, U.H.; Roshani, G.H. Design and Implementation of a Microwave Microstrip Sensor with Convolutional Neural Network for Real-Time Milk Spoilage Detection. *Sens. Int.* **2026**, *7*, 100353. [CrossRef]

11. Morales-Lovera, H.-N.; Olvera-Cervantes, J.-L.; Perez-Ramos, A.-E.; Corona-Chavez, A.; Saavedra, C.E. Microstrip Sensor and Methodology for the Determination of Complex Anisotropic Permittivity Using Perturbation Techniques. *Sci. Rep.* **2022**, *12*, 2205. [CrossRef]
12. Rahimian Omam, Z.; Nayyeri, V.; Javid-Hosseini, S.-H.; Ramahi, O.M. Simple and High-Sensitivity Dielectric Constant Measurement Using a High-Directivity Microstrip Coupled-Line Directional Coupler. *IEEE Trans. Microw. Theory Tech.* **2022**, *70*, 3933–3942. [CrossRef]
13. Karasaeng, W.; Nualkham, J.; Thitimahatthanakusol, P.; Angkawisittpan, N.; Sonasang, S. The Correlation of Pickled Fish and Frequency Response Using Parallel-Coupled-Lines Band-Stop Filter Microstrip. *Eng. Proc.* **2024**, *82*, 13. [CrossRef]
14. Phanomupatum, P.; Phromloungsri, R.; Wongpatsa, D.; Pongthavornkamol, T.; Saeng-On, P.; Sonasang, S. Efficient and Non-Invasive Rice Moisture Quantification Using Coupled Lines Microwave Sensor Design. In Proceedings of the 2024 8th International Conference on Information Technology (InCIT), Chonburi, Thailand, 14–15 November 2024; pp. 473–478. [CrossRef]

Disclaimer/Publisher's Note: The statements, opinions and data contained in all publications are solely those of the individual author(s) and contributor(s) and not of MDPI and/or the editor(s). MDPI and/or the editor(s) disclaim responsibility for any injury to people or property resulting from any ideas, methods, instructions or products referred to in the content.